Coalbed methane adsorption and desorption characteristics related to coal particle size*

Yan-Yan Feng(冯艳艳)[1,2], Wen Yang (杨文)[1,2], and Wei Chu(储伟)[2,†]

[1] *Department of Chemistry and Bioengineering, Guilin University of Technology, Guilin* 541006, *China*
[2] *Department of Chemical Engineering, Sichuan University, Chengdu* 610065, *China*

(Received 1 December 2015; revised manuscript received 28 January 2016; published online 20 April 2016)

Effects of particle size on CH_4 and CO_2 adsorption and desorption characteristics of coals are investigated at 308 K and pressures up to 5.0 MPa. The gas adsorption and desorption isotherms of coals with particle sizes ranging from 250 μm to 840 μm are measured via the volumetric method, and the Langmuir model is used to analyse the experimental results. Coal particle size is found to have an obvious effect on the coal pore structure. With the decrease of coal particle size in the process of grinding, the pore accessibility of the coal, including the specific surface area and pore volume, increases. Hence, coal with smaller particle size has higher specific surface area and higher pore volume. The ability of adsorption was highly related to the pore structure of coal, and coal particle size has a significant influence on coal adsorption/desorption characteristics, including adsorption capacity and desorption hysteresis for CH_4 and CO_2, i.e., coal with a smaller particle size achieves higher adsorption capacity, while the sample with a larger particle size has lower adsorption capacity. Further, coal with larger particle size is also found to have relatively large desorption hysteresis. In addition, dynamic adsorption performances of the samples are carried out at 298 K and at pressures of 0.1 MPa and 0.5 MPa, respectively, and the results indicate that with the increase of particle size, the difference between CO_2 and CH_4 adsorption capacities of the samples decreases.

Keywords: particle size, coalbed methane, adsorption, desorption

PACS: 81.05.U–, 89.30.ag **DOI:** 10.1088/1674-1056/25/6/068102

1. Introduction

With the gradual advent of more and more strict environmental rules, the green energy source serving as a sustainable energy supply is urgently needed.[1] Under this background, coalbed methane (CBM) is becoming an important new energy resource, which could ultimately eliminate gas outburst and reduce environmental pollution. Therefore, the realization of coal and CBM simultaneous extraction is of great significance for improving the efficiency and safety of coal production, reducing greenhouse gas emissions and improving energy efficiency.[2,3] Hence, a better understanding of the relationship between the coal property and gas adsorption capacity can play a significant role in the various areas of the coal mining industry and CBM.[2,4,5]

Furthermore, the ever-increasing CO_2 emissions from fossil-fuel burning by human activities is causing the obvious greenhouse effect and worldwide climate change, and the development of technologies to ease climate change has been one of the biggest challenges.[6] Compared with the technologies to improve the energy efficiency and the use of clean energy combustion, the suitable carbon capture and sequestration (CCS) technologies urgently need developing, and adsorption is a potentially attractive alternative in the context of CCS. Research on CBM adsorption/desorption performances has the vital significance for developing the CBM and CCS.[7] According to CBM adsorption/desorption isotherms, the gas content in coal reservoirs can be estimated to predict the recovery of CBM and the injection rate of carbon dioxide, etc.[8–11]

To date, many researchers have recognized the most important factors influencing gas storage over coals, including coal type,[12–16] rank,[17] moisture content,[18,19] temperature,[20] burial depth,[21,22] pore characteristics,[13,22] etc.[23–32] However, experimental results are still greatly different although the adsorption tests have been used for many years to estimate CBM (mainly methane) storage capacity of coals. The most significant causes of errors are believed to be due to the oxidation of coals and the use of crushed samples that are not representative of the *in situ* conditions.[33] Feng *et al.*[34] have investigated the effects of oxygen-containing groups on methane adsorption by modified coals, and the results showed that the oxidation treatments reduced the ability to adsorb methane over the coals, similar to Hao *et al.*'s results.[30] Zhang *et al.*[35] have studied the influence of the particle size on methane adsorption by coals, and the results showed that with the increase of coal particle size, the adsorption equilibrium time became longer, but the methane adsorption capacity was not affected. However, the study of Xu *et al.*[36] showed that the smaller the coal particle size, the higher the amount of methane is adsorbed, which is consistent with the result of Chu *et al.*[37]

Based on the above description, the effects of particle size on coal pore structure and CBM (CH_4 and CO_2) adsorption/desorption characteristics are investigated in this work.

*Project supported by the National Basic Research Program of China (Grant No. 2011CB201202).
†Corresponding author. E-mail: chu1965chengdu@163.com
© 2016 Chinese Physical Society and IOP Publishing Ltd

The pore structures of coal samples with different particle size distributions are characterized by N_2 adsorption/desorption isotherms at 77 K. The adsorption and desorption isotherms of CH_4 and CO_2 are measured at pressures up to 5.0 MPa by a volumetric method at 308 K, and the Langmuir model is used to fit the experimental data. Furthermore, the dynamic adsorption experiments are performed to study the breakthrough curves of coal samples with various particle size distributions.

2. Experiment

2.1. Preparation

The coal sample used in the present study was from the Sijiazhuang Coalmine, Shanxi, China. Table 1 shows proximate and ultimate analyses of raw coal. Raw coal was dried, crushed and sieved to particle sizes of 250 μm–420 μm and 420 μm–840 μm, respectively. The as-prepared coal particles were dried in an oven overnight at 383 K and stored in sealed plastic containers. The resulting samples were named SJZ-*x*-*y*, where *x* refers to the mass proportion of the coal sample with 420 μm–840 μm and *y* represents the mass ratio for the 250 μm–420 μm coal sample. Therefore, the samples were denoted as SJZ-0-100, SJZ-20-80, SJZ-40-60, SJZ-60-40, SJZ-80-20, and SJZ-100-0, respectively. The samples of various particle sizes were considered in evaluating the effects of particle size on the coal pore structure and CH_4 and CO_2 adsorption/desorption characteristics.

Table 1. Chemical analyses of raw coal (air-dried basis, wt.%).

Coal	Proximate analysis			Ultimate analysis					
	Fixed carbon	Ash	Volatile matter	Moisture	C	H	N	S	O*
Value	61.95	29.31	8.74	0.49	66.54	3.22	< 0.5	2.13	> 27.61

O*: by difference.

2.2. Characterization

The proximate analysis of raw coal was investigated by a GF-A6 automatic proximate analyzer (Hebi Celestica Instruments Co., Ltd).[22,30]

The ultimate analysis of raw coal was performed in a CARLO ERBA 1106 element analyzer (Italy).[30]

X-ray diffraction pattern of raw coal was recorded in DX-1000 powder diffractometer equipped with Cu Kα x-ray source and an internal standard of silicon power.[24,32]

FT-IR analysis of raw coal was performed on a Nicolet DXC20 FT-IR spectrometer.[22]

Thermogravimetric analysis (TG) of raw coal was carried out on a thermo gravimetric analyzer (TGA Q500). The samples were heated at a rate of 10 °C/min under N_2 atmosphere.[32]

Surface morphology of raw coal was investigated by scanning electron microscopy (SEM) (JEOL/EO JSM-5900 microscope).[1]

The textural properties of the samples with varying particle sizes were obtained by N_2 adsorption/desorption isotherms, determined at 77 K with a NOVA1000e surface area and pore size analyzer (Quantachrome Company).[1,34,35]

2.3. Gas adsorption and desorption measurements

Gas adsorption and desorption measurements were performed by a volumetric method similar to that previously described.[22,24,30,32] Approximately 5-g coal was dried at 110 °C and evacuated for 3 h, prior to the determination of void volume in the adsorption setup by helium calibration. Subsequent to helium calibration, the samples were again evacuated for 3 h. CH_4 or CO_2 was introduced into the adsorption setup to produce an adsorption isotherm under pressures up to 5.0 MPa at 308 K. The test was repeated three times and the mean value of the equilibrium data was used to calculate the adsorption isotherm to ensure the validity of the experiment.

2.4. Dynamic gas adsorption tests

Dynamic gas adsorption test was carried out with about 20.0-g coal at 298 K under 0.5 MPa and 0.1 MPa, respectively. Prior to measurement, the coal sample was dried at 110 °C overnight. The content of He/CO_2/CH_4 used in the experiment was 55.08:6.07:38.85 (volume ratio, %).

3. Results and discussion

3.1. Structural properties of raw coal

The structural properties of raw coal are characterized by XRD, FT-IR, TG and SEM techniques, respectively. Figure 1(a) shows the XRD pattern of raw coal. There exists a broad peak at around 25°, attributed to the (002) characteristic plane of graphite. FT-IR profile for raw coal is shown in Fig. 1(b). An absorption band appears at around 3400 cm^{-1}, assigned to –OH stretching. The adsorption peaks observed at 2900 cm^{-1}–3000 cm^{-1} and 1670 cm^{-1}–1760 cm^{-1} are attributed to –COOH group vibrations. The peak appearing at 1000 cm^{-1}–1200 cm^{-1} can be attributed to esters, such as those in ethers, phenols and hydroxyl groups. Shoulder bonds at low wavenumbers (< 1000 cm^{-1}) may be related to out-of-plane bending modes. Figure 1(c) displays the normalized weight change of raw coal due to the heat treatment from

100 °C to 750 °C under N_2 atmosphere. Dehydration mainly happens below 350 °C, together with small evolutions of other gases. In a temperature range of 400 °C–750 °C, extensive evolution of hydrocarbons that correspond to volatile organic components takes place. As confirmed in Fig. 1(c), the weight loss for raw coal SJZ due to heat treatment is 8.43%, which is consistent with the proximate analysis results. Figure 2 shows the SEM images of raw coal, which exhibits a dense structure with an irregular, heterogeneous and porous surface, illustrating the development of micropores.

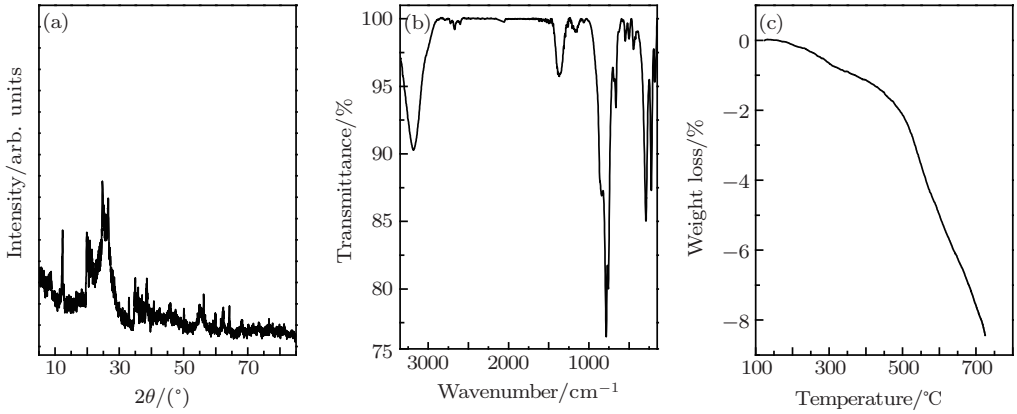


Fig. 1. XRD profile (a), FT-IR (b), and weight loss (c) of raw coal SJZ.

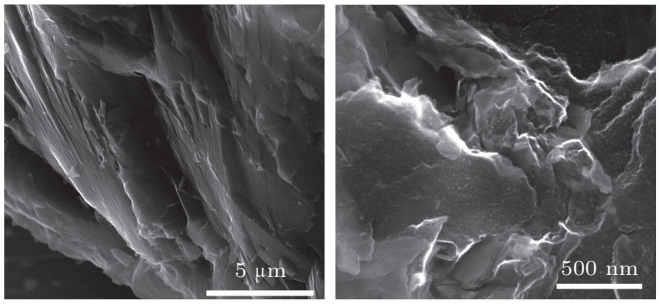


Fig. 2. SEM images of raw coal SJZ.

3.2. Pore structure characteristics of the samples

As a key parameter, the pore structure, which includes the specific surface area, pore volume and pore size distribution, directly affects the CBM production. Based on the knowledge of the nature of coal and its pore system, N_2 adsorption/desorption, could characterize the pore structure.[22]

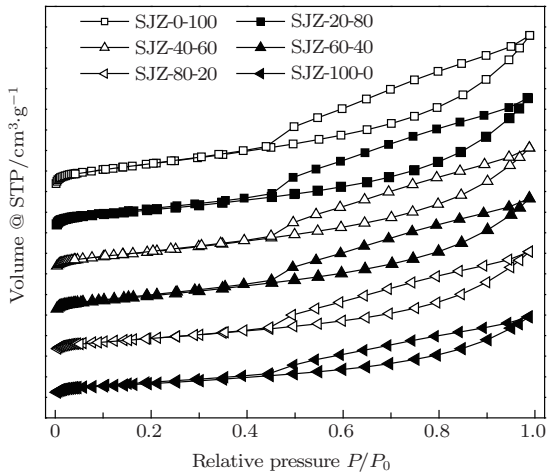


Fig. 3. N_2 adsorption/desorption isotherms at 77 K of the coal samples.

Figure 3 displays N_2 adsorption/desorption isotherms at 77 K as a function of coal particle size. According to the BET classification, the adsorption isotherms of this kind belong to type III describing the physical adsorption process of N_2. The isotherms exhibit the remarkable hysteresis loops at higher relative pressures ($P/P_0 > 0.45$). It is obvious that the nitrogen adsorption volume of sample SJZ-0-100 is the highest among the six samples, while the adsorption volume of SJZ-100-0 is the lowest.

Table 2. Textural characteristics of the coal samples.

Sample	Specific surface area[a]/(m^2/g)	Pore volume[b] (10^{-3} cm^3/g)	PD[c]/nm
SJZ-0-100	5.267	10.380	3.794
SJZ-20-80	3.329	8.950	3.969
SJZ-40-60	3.110	8.354	3.969
SJZ-60-40	2.881	7.718	3.969
SJZ-80-20	2.532	6.902	3.969
SJZ-100-0	1.988	5.325	4.152

[a]Measured from NLDFT method. [b]Evaluated from NLDFT method.
[c]Average pore diameter calculated from NLDFT method.

Table 2 presents the corresponding textural characteristics related to the specific surface area (SSA), pore volume (PV), and average pore diameter (PD). The variation of coal particle size leads to differences in SSA, PV, and PD. Among the samples, SJZ-0-100 with the smallest particle size displays the highest SSA and PV, indicating that the porosity of SJZ-0-100 is developed in the grinding process, which possibly opens some closed pores, leading to an increased pore accessibility. Compared with the others, the sample SJZ-100-0 has a low SSA of 1.988 m^2/g and PV of 5.325×10^{-3} cm^3/g.

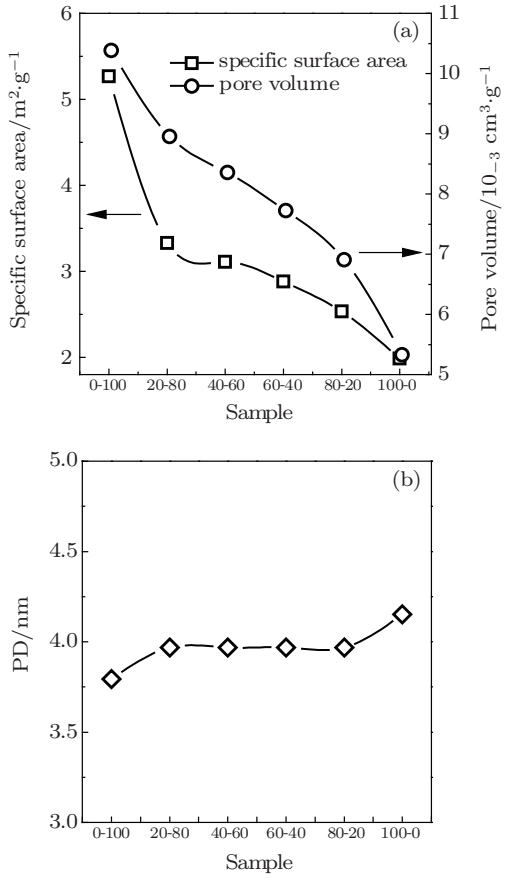


Fig. 4. Relationships between the textural characteristics and particle size distribution of the samples.

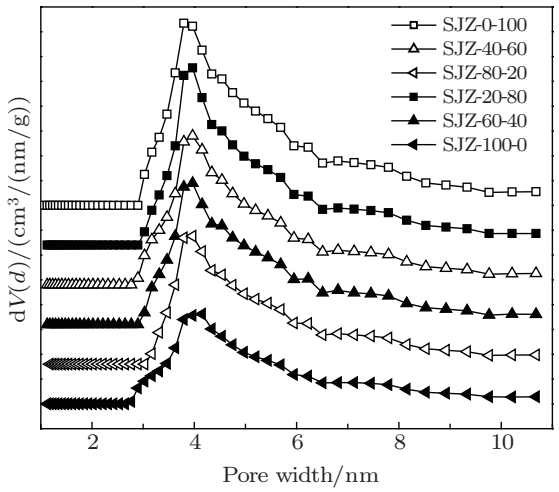


Fig. 5. Pore size distributions obtained by applying the DFT equation for the coals.

Figure 4 shows the textural characteristics as a function of coal particle size. It can be seen that the sample SJZ-100-0 with the largest coal particle size has a total SSA of 1.988 m^2/g, and after being ground into smaller particles, the total SSAs increase up to 2.532 m^2/g for SJZ-80-20, 2.881 m^2/g for SJZ-60-40, 3.110 m^2/g for SJZ-40-60, 3.329 m^2/g for SJZ-20-80, and 5.267 m^2/g for SJZ-0-100, respectively. At the same time, with the particle size decreasing, the PV increases, while PD decreases. This result shows that the coal sample with reduced particle size has an increased pore accessibility and consequently an increase in the nitrogen amount adsorbed, thus leading to the increases of SSA and PV.

Figure 5 displays the pore size distributions of the samples obtained by applying the DFT method, from which the difference in micropores size distributions among the samples can be clearly seen. Apparently, the decrease of coal particle size can increase the volumes of micropores.

3.3. Gas adsorption and desorption performances

Figure 6(a) shows the measured data of CH_4 adsorption on the samples at 308 K under pressures up to 5.0 MPa. The CH_4 adsorption isotherms belong to type I of IUPAC. Differences in coal particle size and SSA can result in variation of CH_4 adsorption capacity. The adsorption capacity over coal increases with particle size reducing. Among the samples, the sample SJZ-0-100 possesses the highest methane adsorption capacity while the SJZ-100-0 sample has the lowest methane adsorption capacity.

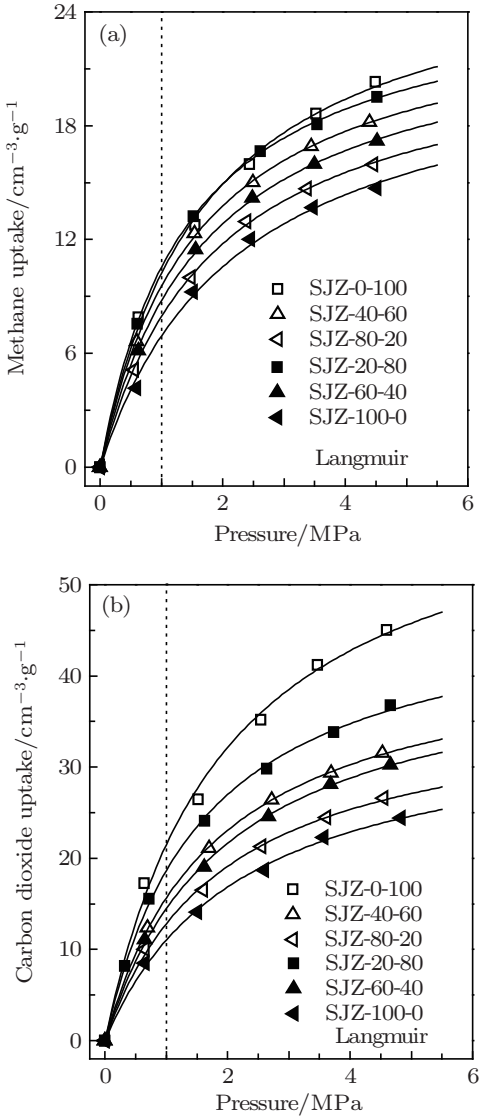


Fig. 6. CH_4 (a) and CO_2 (b) adsorption isotherms of the coal samples, obtained by applying the Langmuir model (solid lines) at 308 K.

Figure 6(b) exhibits CO_2 adsorption abilities of the samples evaluated by a volumetric method at 308 K. The CO_2 adsorption isotherms display a zoom at the low pressure region. As expected, the smaller particle size coal sample has a much higher CO_2 uptake than the larger particle size sample due to its developed pore structure. Since the structural properties are significantly affected by coal particle size, it is possible to enhance CO_2 uptake in a certain range.

Table 3. Adsorption parameters obtained from Langmuir model of the coal samples.

Sample	CH_4			CO_2		
	V_L/(cm^3/g)	b/MPa^{-1}	R^2	V_L/(cm^3/g)	b/MPa^{-1}	R^2
SJZ-0-100	27.686	0.585	0.99750	63.818	0.508	0.99506
SJZ-20-80	25.648	0.698	0.99981	48.810	0.618	0.99886
SJZ-40-60	24.752	0.628	0.99974	43.926	0.553	0.99978
SJZ-60-40	23.856	0.581	0.99956	42.896	0.518	0.99937
SJZ-80-20	22.781	0.535	0.99967	37.565	0.509	0.99846
SJZ-100-0	22.422	0.445	0.99678	35.638	0.448	0.99792

Because of its simplicity and providing a reasonable fit to most experimental data, the Langmuir model is widely used in the CBM industry and relevant reservoir simulations. Hence, in the present work the Langmuir model is used to fit the adsorption data, which fits experimental results quite well ($R^2 > 0.99$). The adsorption parameters of the Langmuir model are listed in Table 3.

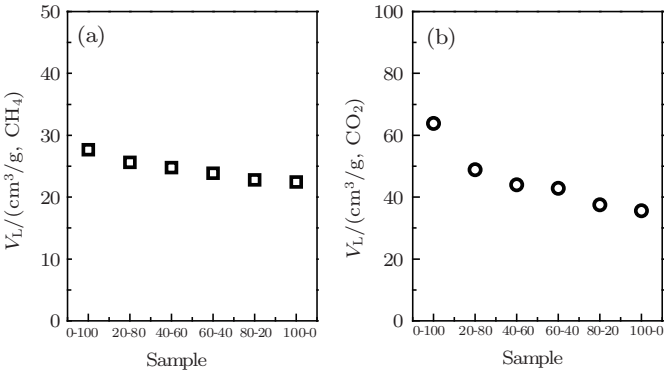


Fig. 7. Relationships between maximum adsorption capacity of CH_4 (a) and CO_2 (b) and particle size distributions of the samples.

The parameter V_L in the model is the maximum uptake of the adsorbent, and b is the reciprocal of the pressure when the adsorption capacity reaches 50% of the maximum uptake. The values of maximum adsorption capacity (V_L) of the coal samples vary from 22.422 cm^3/g to 27.686 cm^3/g for CH_4 and from 35.638 cm^3/g to 63.818 cm^3/g for CO_2, respectively. It reveals that the particle size has a significant effect on the gas adsorption capacity for the coal samples, i.e., the gas adsorption capacity increases as the coal particle size decreases. From Fig. 7, it can be clearly seen that the maximum adsorption capacities of CH_4 and CO_2 both decrease with the coal particle size increasing, but the declining trend of CO_2 maximum adsorption amount is more obvious than that of CH_4.

Figure 8 shows the relationships between Langmuir constant b and particle size of the coals. As shown in Fig. 8, the particle size has the different effects on Langmuir constant b for the coal samples. For the coal samples ranging from SJZ-0-100 to SJZ-20-80, the Langmuir constant b increases, however, for the coal with larger particle size the parameter b decreases, which means a weaker adsorbent/adsorbate interaction.

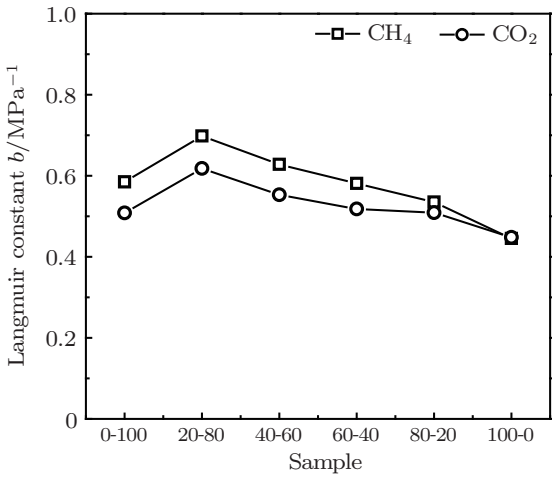


Fig. 8. Relationships between Langmuir constant b and particle size of the coals.

Figure 9 shows CH_4 adsorption/desorption isotherms of the coals. It can be seen that the adsorption/desorption isotherms of the tested coals have apparent hystereses for all coal particle sizes. The phenomenon that desorption isotherms generally lie above the adsorption isotherms represents that the adsorption hysteresis is associated with the adsorption/desorption process. Coal, as the adsorbent, when adsorbing and desorbing the adsorbate, produces the hysteresis, which not only happens to gas, but also to water. The hysteresis effect indicates that the adsorbent/adsorbate system is in a metastable state and at reducing pressure the gas is not readily released to the extent corresponding to the thermodynamic equilibrium value.

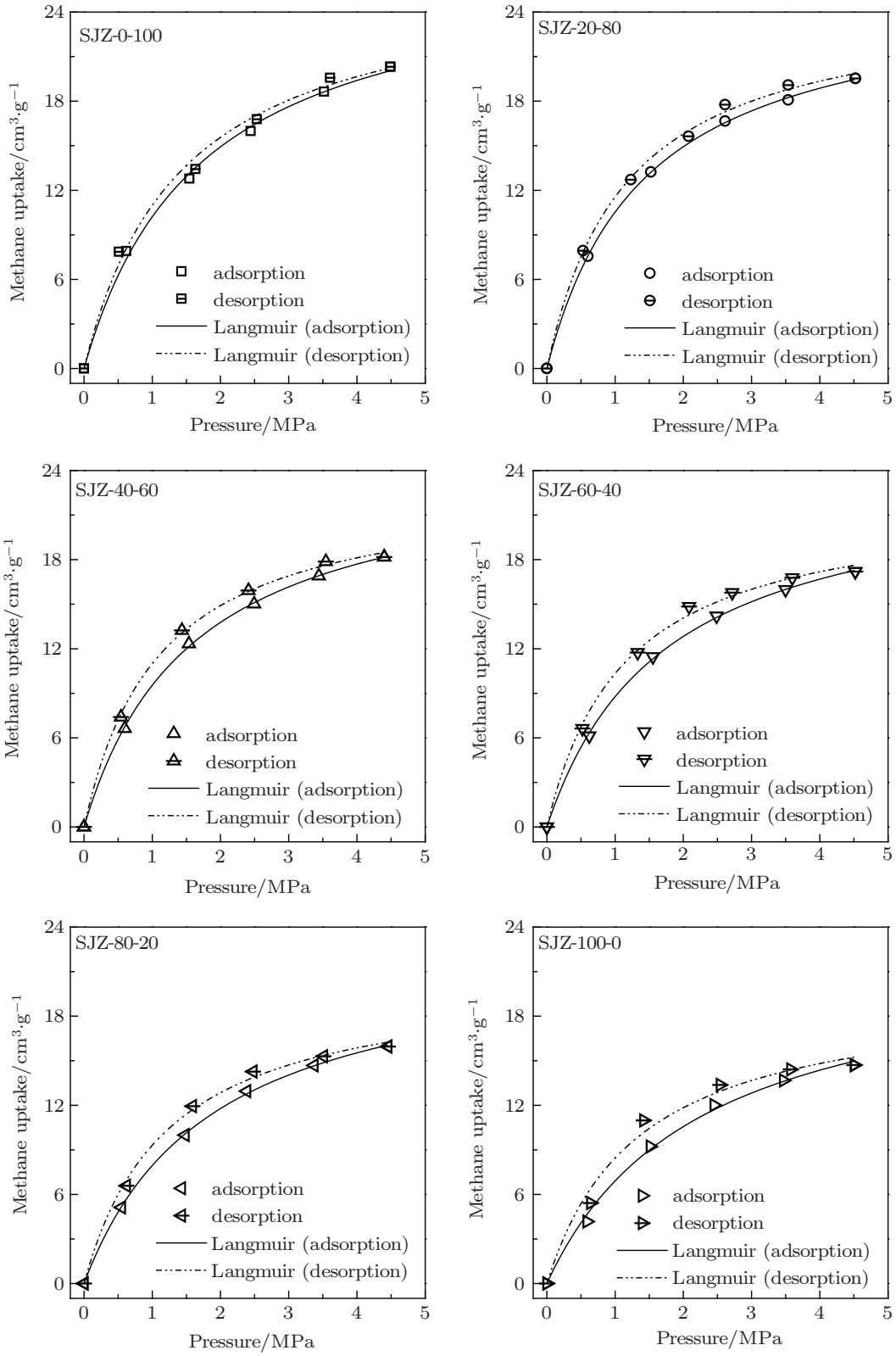


Fig. 9. CH_4 adsorption/desorption isotherms of the coals.

Figure 10 demonstrates CO_2 adsorption/desorption isotherms of the coals, in which the adsorption/desorption hysteresis is similar to that of CH_4. The existence of the hysteresis could be explained by the nature of CO_2 adsorption over the coal. As shown in Fig. 10, larger particle size coal gives rise to a larger hysteresis. Coal with larger particle size has a better chance to trap the gas molecules as it possesses longer path distances for gas to be desorbed from the internal surface. CO_2 molecules may be absorbed/dissolved into the coal structure[38] and when the desorption process happens, only the adsorbed molecules come out of the pore-spaces leaving behind the dissolved molecules in the coal structure.

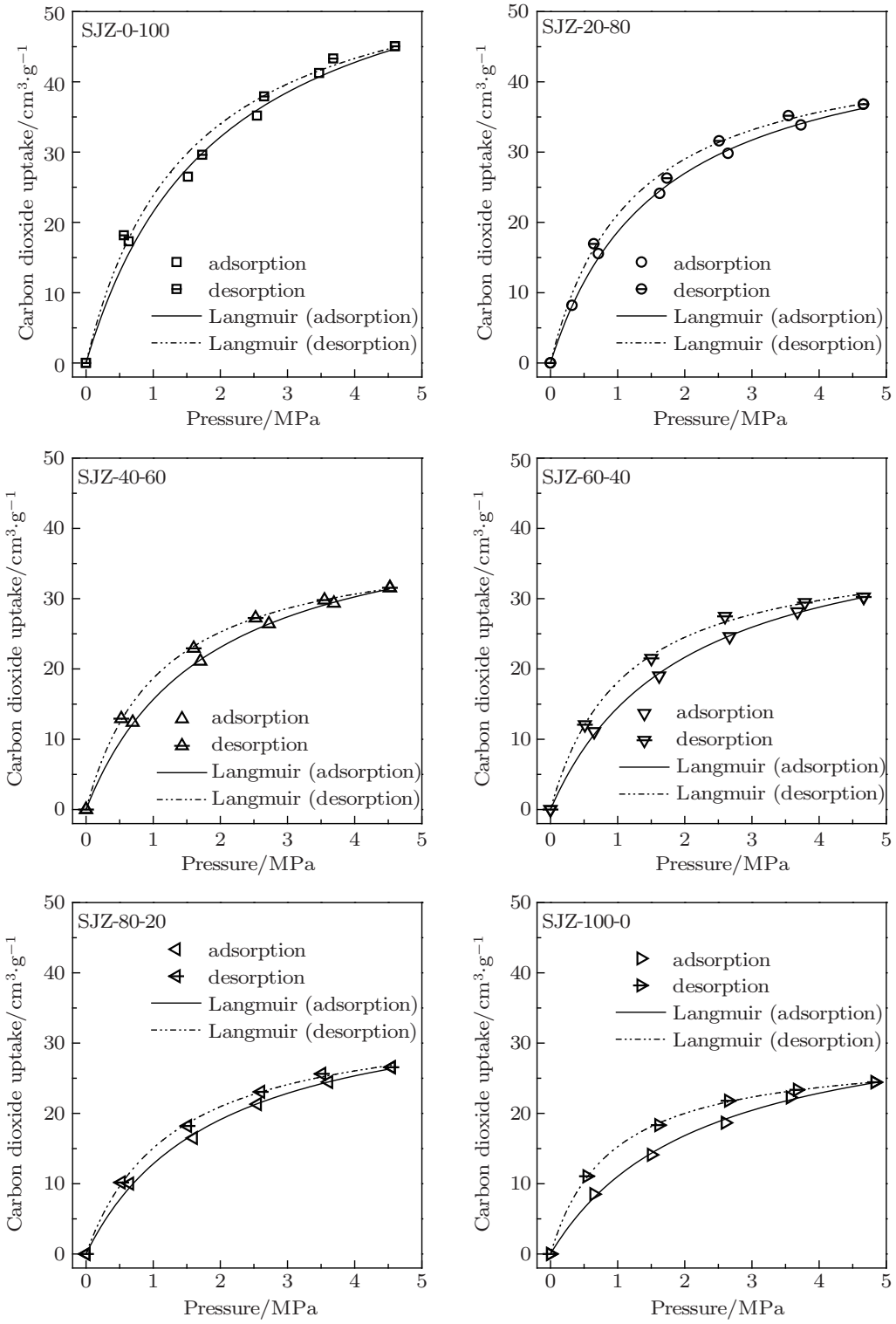


Fig. 10. CO_2 adsorption/desorption isotherms of the coals.

The ratio of the maximum adsorption capacities $V_{L(CO_2)}/V_{L(CH_4)}$ derived from adsorption and desorption isotherms is consistently greater than 1, reflecting the preferential adsorption of CO_2 compared with CH_4 and implicating the feasibility of CO_2 enhanced methane recovery (CO_2-ECBM). From Fig. 11, the ratio of $V_{L(CO_2)}/V_{L(CH_4)}$ diminishes with coal particle size increasing, and thus the degree of preferential adsorption for CO_2 decreases. With the increase of coal particle size, the selectivity for CO_2 adsorption decreases, which is in line with the trend of $V_{L(CO_2)}$. In the adsorption process, $V_{L(CO_2)}/V_{L(CH_4)}$ is in a range of 1.588–2.306, while $V_{L(CO_2)}/V_{L(CH_4)}$ varies between 1.468 and 2.236 in the desorption process, i.e., the trends for $V_{L(CO_2)}/V_{L(CH_4)}$ along with coal particle size in both adsorption and desorption processes are similar.

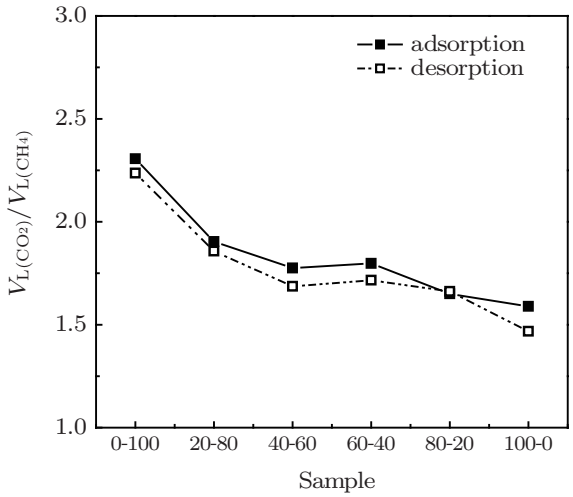


Fig. 11. Ratios of the maximum uptake for CO_2/CH_4.

3.4. Dynamic gas adsorption performances

Figure 12 displays CH_4 and CO_2 breakthrough curves of the coal sample SJZ-0-100 at 298 K under pressures of 0.1 MPa and 0.5 MPa, respectively. As seen from Fig. 12, CH_4 has a shorter breakthrough time than CO_2, and with pressure increasing from 0.1 MPa to 0.5 MPa, the adsorption equilibrium time becomes longer. When the pressure is 0.1 MPa, the breakthrough times of CH_4 and CO_2 are 11 s and 16 s respectively, but as the pressure increases up to 0.5 MPa, the breakthrough times change into 42 s and 108 s respectively, indicating that the difference in breakthrough time between CH_4 and CO_2 is more obvious, for the increasing of pressure will increase the density of gas molecules, thereby improving the interaction between the adsorbate and the coal, which in turn enhances the gas adsorption capacity.

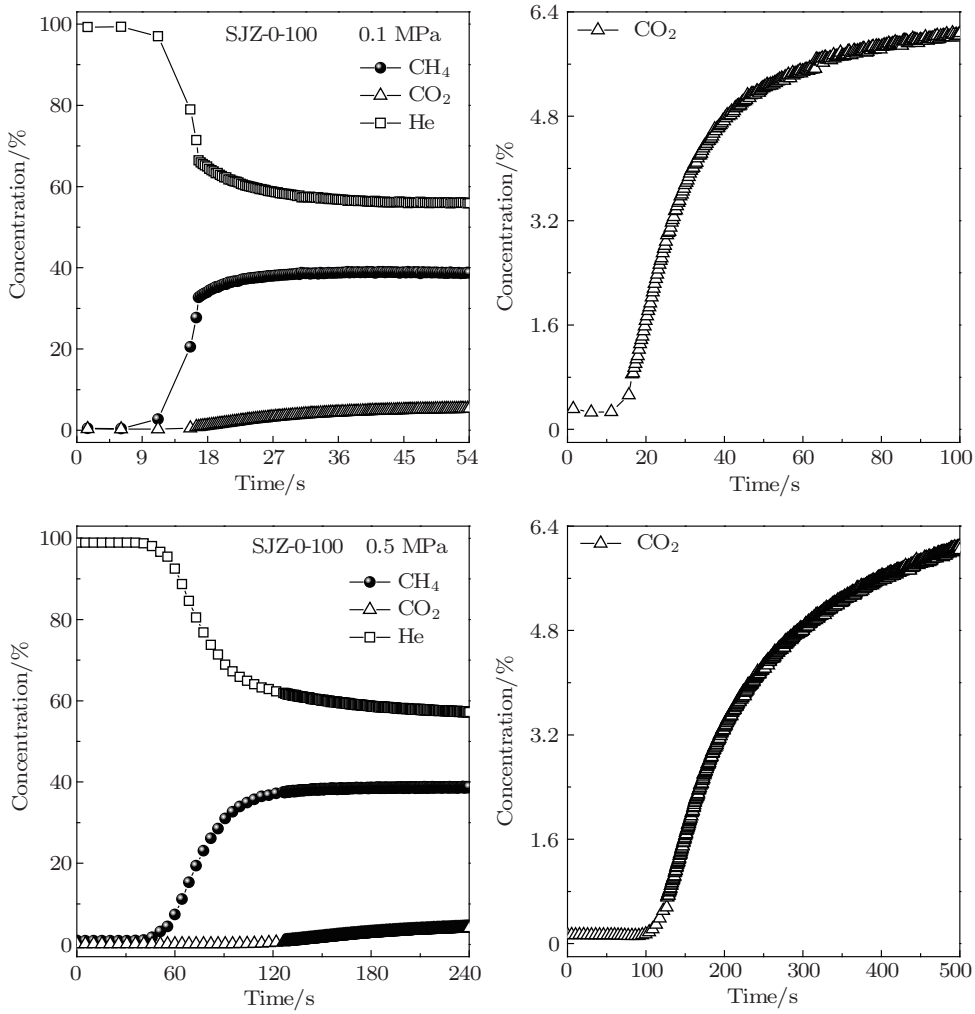


Fig. 12. Breakthrough curves of He, CO_2, and CH_4 on the coal sample SJZ-0-100 at 298 K under different pressures.

Figure 13 shows breakthrough curves of CO_2 and CH_4 on the typical samples SJZ-0-100 and SJZ-100-0 at 0.5 MPa. The smaller particle size sample SJZ-0-100 has a higher breakthrough time, i.e., the adsorption amount of the SJZ-0-100 sample is higher. The breakthrough times of CH_4 and CO_2 for the sample SJZ-0-100 are 42 s and 108 s, and their difference is 66 s. As particle size increases, the breakthrough times of the sample SJZ-100-0 are shortened, i.e., 39 s for CH_4 and 77 s for CO_2, and the difference in breakthrough time between the CO_2 and CH_4 becomes 38 s. The shorter breakthrough time indicates that the

gas uptake of the adsorbent is smaller. Hence, according to the decrease of the breakthrough time difference, it is demonstrated that the increase of particle size makes the ratio of V_{CO_2}/V_{CH_4} reduced, which is consistent with the results indicated in Figs. 11 and 14.

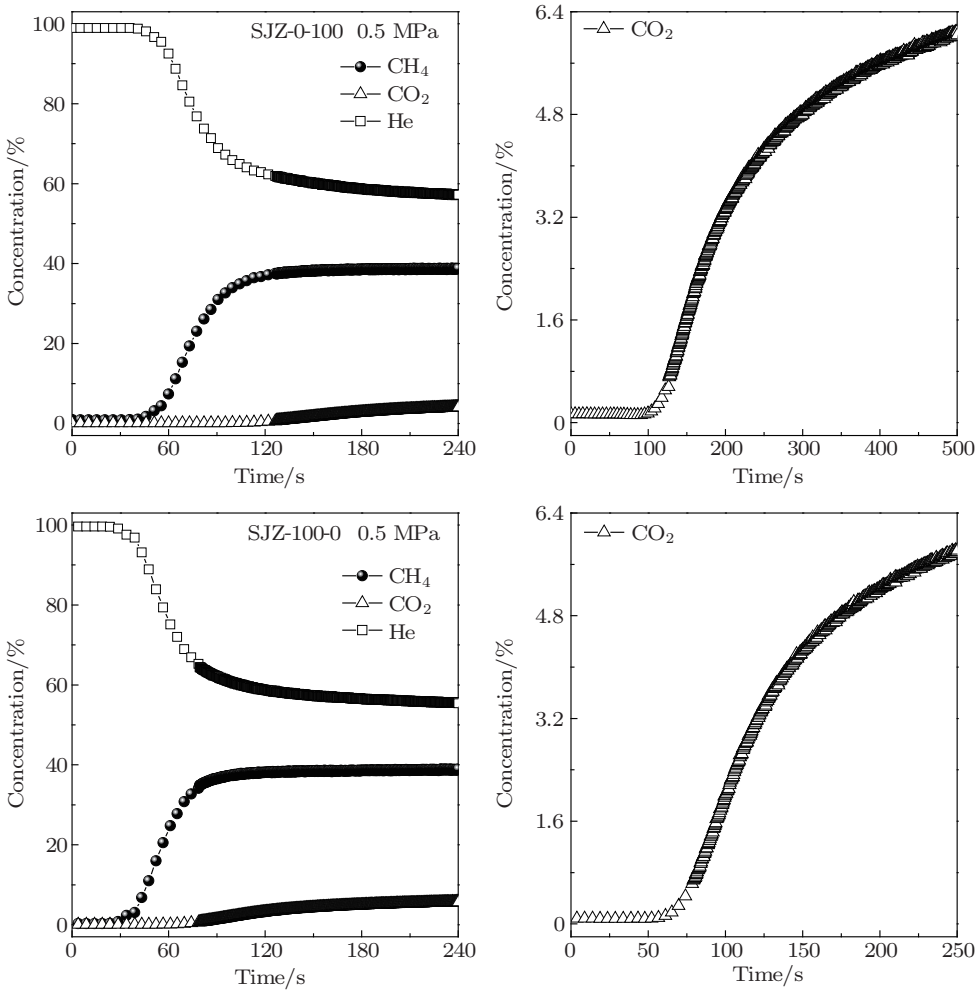


Fig. 13. Breakthrough curves of He, CO_2, and CH_4 on the typical samples SJZ-0-100 and SJZ-100-0 at 0.5 MPa.

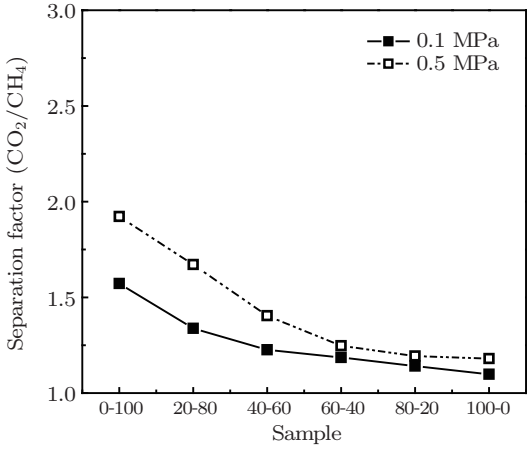


Fig. 14. Separation factors of CO_2/CH_4 versus coal sample under pressures of 0.1 MPa and 0.5 MPa.

4. Conclusions

Gas adsorption and desorption behaviors on coals with varying particle sizes are studied in this work. The adsorption and desorption characteristics of CH_4 and CO_2 are investigated at 308 K and pressures up to 5.0 MPa by a volumetric method. Dynamic adsorption tests of the samples are carried out at 298 K and at pressures of 0.1 MPa and 0.5 MPa, respectively. The experimental data are fitted by the Langmuir model, and the fitting results show that the Langmuir model fits the data well. The gas adsorption on coals is related to their physical structures and particle sizes. As a result, there is a positive correlation with the particle size and the SSA and PV of samples, i.e., coal with smaller particle size has higher SSA, higher PV and lower PD.

Coal particle size is correlated strongly with CH_4 and CO_2 adsorption capacities. Langmuir volume V_L decreases with coal particle size increasing, and the difference in $V_{L(CH_4)}$ among coal samples with various particle sizes is smaller than that of CO_2. The adsorption and desorption isotherms have apparent hystereses for both CH_4 and CO_2, caused by all range of particle size coals, and larger particle size coals show a larger

hysteresis. The difference in $V_{L(CH_4)}/V_{L(CO_2)}$ becomes smaller with increasing coal particle size, and thus the degree of preferential adsorption of CO_2 is reduced. The dynamic adsorption results indicate that with the increase of coal particle size, the differences in adsorption capacity between CO_2 and CH_4 decreases, which is in good agreement with the results of the gas adsorption and desorption characteristics.

References

[1] Yang W, Feng Y Y, Xiao D and Yuan H Y 2015 *Int. J. Energ. Res.* **39** 805
[2] Zhang S I, Huo Y Z, Ye J P, Tang S H and Ma D M 2005 *Chin. Sci. Bull.* **50** 158
[3] Zhao Y and Peng H Y 2013 *Disa. Adv.* **6** 291
[4] Lin D Y, Ye J P, Qin Y and Tang S H 2000 *Acta Geol. Sin.-Engl.* **74** 706
[5] Zhang D F, Gu L L, Li S G, Lian P C and Tao J 2013 *Energ. Fuel* **27** 387
[6] Zheng J J, Zhou Y P, Zhi Y T, Su W and Sun Y 2012 *Adsorption* **18** 121
[7] Harpalani S, Prusty B K and Dutta P 2006 *Energ. Fuel* **20** 1591
[8] Ottiger S, Pini R, Storti G and Mazzotti M 2008 *Adsorption* **14** 539
[9] Jodłowski G S, Baran P, Wójcik M, Nodzeński A, Porada S and Milewska-Duda J 2007 *Appl. Surf. Sci.* **253** 5732
[10] Ziarani A S, Aguilera R and Clarkson C R 2011 *Fuel* **90** 2428
[11] Lafortune S, Adelise F, Bentivegna G, Didier C, Farret R, Gombert P, Lagnya C, Pokryszkaa Z and Toimil N C 2014 *Energ. Procedia* **63** 5870
[12] Nie B S, Liu X, Yang L, Meng J and Li X 2015 *Fuel* **158** 908
[13] Liu H, Mou J and Cheng Y 2015 *J. Nat. Gas Sci. Eng.* **22** 203
[14] Nie B S, Yang T, Li X C, Li L and Lu H Q 2013 *J. China Univ. Min. Technol.* **42** 975 (in Chinese)
[15] Weishauptova Z and Sykorova I 2011 *Fuel* **90** 312
[16] Garnier C, Finqueneisel G, Zimny T, Pokryszka Z, Lafortune S, Defossez P D C and Gaucher E C 2011 *Int. J. Coal Geol.* **87** 80
[17] Zhang D F, Cui Y J, Liu B, Li S G, Song W L and Lin W G 2011 *Energ. Fuel* **25** 1891
[18] Ozdemir E and Schroeder K 2009 *Energ. Fuel* **23** 2821
[19] Nie B S, Liu X F, Guo J H and Zhu F F 2015 *J. China Univ. Min. Technol.* **44** 781 (in Chinese)
[20] Zhao D, Zhao Y S, Feng Z C, Liu Z X and Liu T 2012 *Energ. Source Part A* **34** 324
[21] Sun W J, Feng Y Y, Jiang C F and Chu W 2015 *Fuel* **155** 7
[22] Feng Y Y, Jiang C F, Liu D J and Chu W 2014 *Chin. Phys. B* **23** 028201
[23] Hou Q L and Li X S 2014 *Physics* **43** 373 (in Chinese)
[24] Feng Y Y, Yang W and Chu W 2014 *Chin. Phys. B* **23** 108201
[25] Yan J, Xu W Y, Guo H, Gong Y, Mi Y M and Zhao X X 2015 *Acta Phys. Sin.* **64** 016802 (in Chinese)
[26] Liang J Q, Liang Z Z, Zhu W B and Su F G 2011 *Acta Phys. Sin.* **60** 057802 (in Chinese)
[27] Cygankiewicz J, Dudzinska A and Zyla M 2007 *Arch. Min. Sci.* **52** 573
[28] Zhang D F, Li S G, Cui Y J, Song W L and Lin W G 2011 *Ind. Eng. Chem. Res.* **50** 8742
[29] Cui Y J, Zhang D F, Zhang Q, Lin W G, Song W L, Li Y H and Jiang W P 2010 *Acta Geol. Sin.-Engl.* **84** 1547
[30] Hao S X, Wen J, Yu X P and Chu W 2013 *Appl. Surf. Sci.* **264** 433
[31] Weniger P, Francu J, Hemza P and Krooss B M 2012 *Int. J. Coal Geol.* **93** 23
[32] Feng Y Y, Jiang C F, Liu D J and Chu W 2013 *J. Anal. Appl. Pyrol.* **104** 559
[33] Fitzgerald J E, Pan Z, Sudibandriyo M, Robinson R L, Gasem K A M and Reeves S 2005 *Fuel* **84** 2351
[34] Feng Y Y, Yang W, Liu D J and Chu W 2013 *Chin. J. Chem.* **31** 1102
[35] Zhang X D, Sang S X, Qin Y, Zhang J and Tang J X 2005 *J. China Univ. Min. Technol.* **34** 427 (in Chinese)
[36] Xu J, Liu D, Peng S, Wu X and Lu Q 2010 *Chin. J. Rock Mech. Eng.* **29** 1231
[37] Wang C Y, Hao S X, Sun W J and Chu W 2012 *Int. J. Min. Sci. Technol.* **22** 855
[38] Yang K, Lu X, Lin Y and Neimark A V 2010 *Energ. Fuel* **24** 5955